Enhanced performance of a reservoir computer using polarization dynamics in VCSELs

Jeremy Vatin, Damien Rontani, Marc Sciamanna

Enhanced performance of a reservoir computer using polarization dynamics in VCSELs

Jeremy Vatin[1,2,*], Damien Rontani[1,2], and Marc Sciamanna[1,2]

[1] *Chair in Photonics, CentraleSupélec and Université Paris-Saclay, 2 rue Edouard Belin, 57070 Metz, France*
[2] *LMOPS EA-4423 Laboratory, CentraleSupélec and Université Lorraine, 2 rue Edouard Belin, 57070 Metz, France*
[*] *jeremy.vatin@centralesupelec.fr*

October 16, 2018

We analyze the performance of a reservoir computer based on time delayed feedback and optical injection, which is drawing benefits from the high-speed polarization dynamics of a Vertical Cavity Surface Emitting Laser (VCSEL). We demonstrate that such a system has high computation performance and yields deeper memory than existing single-mode laser-based reservoir computer. Performance is demonstrated on several benchmarking tasks. In particular, the error rate is an order of magnitude smaller when performing channel equalization.

Keywords : *Neural networks, Vertical cavity surface emitting lasers, Optical data processing, Ultrafast technology, Semiconductor lasers*

The growing amount of exchanged information in optical network makes data processing one of today's most critical issue [1]. Neuro-inspired architectures raise interest as a novel approach to process signal, including so-called reservoir computer. Reservoir computing is a technique of machine learning that trains artificial neural networks with recurrent connections by performing regression on a readout layer [2]. Several architectures have been demonstrated such as coupled photonic emitters [3] or silicon photonic reservoir [4]. However having a fully implemented reservoir computer with a high number of nodes remains a technological challenge.

A reservoir architecture using a time-delayed feedback is a particularly promising solution to address this issue [5]. The advantage is that the number of nodes can be easily increased since those are only virtually positioned along the feedback loop. This architecture has shown convincing performance whatever the physical nature of the processed information; i.e. opto-electronic [6, 7] or optical [8–10]. The limitation of the time delay approach is its processing speed, due to the length of the delay line. Using a Vertical Cavity Surface Emitting Laser (VCSEL) can be a solution to that problem, while further improving the computational accuracy. When comparing with conventional edge-emitting lasers, VCSELs exhibit high-speed modulation capability, hence hopefully faster computation, but also the capability to emit coherent light along two coupled polarization modes, which leads to much coupled information generated in the same amount of time [11]. Added to that, VCSELs are already used in telecommunication transmission, that would ease the interface between the current network and our data processing device.

In this letter, we analyze numerically a photonic reservoir computer based on VCSEL and demonstrate that using the two-polarization modes dynamics of a VCSEL improves the performance in terms of speed and accuracy. Our new design is based on delayed optical feedback and optical injection. After showing its computational performance, we prove that it is also efficient in dealing with several benchmarking tasks including the very demanding channel equalization.

We consider an all-optical reservoir computer with time-delayed feedback. The main difference between our system and the ones considered in the literature so far is that our computation node strength relies on the two-mode polarization dynamics of a VCSEL (Fig. 1).

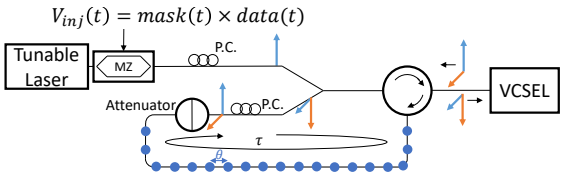

Figure 1: *(color online) Scheme of the photonic reservoir. The dominant (depressed) polarization mode is represented by the blue (orange) arrow. A polarization rotating optical feedback reinjects each polarization mode after rotating it by 90°*

The input (data to be processed) is optically injected thanks to a laser beam which is modulated through a Mach-Zehnder modulator. This modulated-beam is injected in the VCSEL along the main lasing polarization axis. The output of that laser is then sent to a τ-length delay-loop, before being reinjected in the VCSEL. Along the loop, the signal is rotated by $\frac{\pi}{2}$ thanks to a polarization controller (P.C.) in order to trigger lasing in the normally depressed lasing axis, and is attenuated in order to control the feedback strength. Because of that rotation, the depressed mode is injected in the main lasing polarization mode, and the main polarization mode is rotated and injected in the normally suppressed polarization mode. The output layer of our reservoir is composed of virtual nodes, which are positioned along the delay-loop. The time between each two nodes is here called θ. That definition leads us to the following relationship between θ and τ: $\tau = number\ of\ nodes \times \theta$. As in [5], the time discrete input $u(k)$ is convoluted with a mask, which is composed of as many values as the number of nodes, randomly taken between either -1 or 1. Each value of the mask is hold during θ so that the total mask duration is τ.

In order to simulate our system, we consider the SFM model [12, 13] with a feedback term and an optical injection term:

$$\begin{aligned}
\dot{E}_x &= \kappa(1+i\alpha)[(N-1)E_x + inE_y] - (\gamma_a + i\gamma_p)E_x \\
&\quad +\Phi_x(t) + \kappa A_{inj}(t)e^{(\omega_{inj}-\omega_0)t} + F_x(t), \qquad (1)\\
\dot{E}_y &= \kappa(1+i\alpha)[(N-1)E_y - inE_x] + (\gamma_a + i\gamma_p)E_y \\
&\quad +\Phi_y(t) + F_y(t), \qquad (2)\\
\dot{N} &= -\gamma_N[N - \mu + N(|E_x|^2 + |E_y|^2) \\
&\quad +in(E_yE_x^* - E_xE_y*)], \qquad (3)\\
\dot{n} &= -\gamma_s n - \gamma_N[n(|E_x|^2 + |E_y|^2 \\
&\quad +iN(E_yE_x^* - E_xE_y^*)], \qquad (4)
\end{aligned}$$

where E_x and E_y are the values of the orthogonal linearly polarized optical field, N is the population difference between conduction and valence bands n the population difference between the carrier densities with positive and negative spin values and μ is the injection current normalized to threshold. κ is the field decay rate, α is the linewidth enhancement factor, γ_N is the decay rate of the carrier population and γ_s is the decay rate which influences the the mixing of career populations between the two different spins. ω_0 is the pulsation of the self-emitting slave laser, and η is the feedback strength. $A_{inj} = \sqrt{P_{inj}}/2 \times (1 + e^{iV/V_\pi})$ is the value of the injected optical field where P_{inj} is the power of the tunable laser and V is the voltage relative to the input taken within $[-\pi V_\pi; \pi V_\pi]$, ω_{inj} is the pulsation of the master laser. We fix $\kappa = 300$ GHz, $\alpha = 3$, $\gamma_a = -0.1$ GHz, $\gamma_p = 6$ GHz, $\gamma_N = 1$ GHz, $\gamma_s = 50$ GHz, and $\omega_{inj} = \omega_0 = 2\pi f\frac{c}{\lambda}$, where c is the speed of light and $\lambda = 1550$ nm is the wavelength. F_x and F_y are two Langevin noise sources modelling the spontaneous emission noise [14]: $F_x = \sqrt{\frac{\beta_{sp}}{2}}\left(\sqrt{N+n}\xi_1 + \sqrt{N-n}\xi_2\right)$, and $F_y = -i\sqrt{\frac{\beta_{sp}}{2}}\left(\sqrt{N+n}\xi_1 - \sqrt{N-n}\xi_2\right)$, where ξ_1 and ξ_2 are complex Gaussian white noise, and β_{sp} is the spontaneous emission factor. We first consider a deterministic case i.e. $\beta_{sp} = 0$.
Finally, $\Phi_x(t)$ and $\Phi_y(t)$ are the feedback terms. We are considering in this paper two different kinds of feedback, isotropic feedback (IF) and rotated feedback(RF) described as follows:

$$\begin{aligned}
IF: \quad & \Phi_x(t) = \eta E_x(t-\tau)e^{-i\omega_0\tau} \\
& \Phi_y(t) = \eta E_y(t-\tau)e^{-i\omega_0\tau}, \qquad (5)\\
RF: \quad & \Phi_x(t) = -\eta E_y(t-\tau)e^{-i\omega_0\tau} \\
& \Phi_y(t) = \eta E_x(t-\tau)e^{-i\omega_0\tau}. \qquad (6)
\end{aligned}$$

To evaluate the reservoir performance, we analyze two task-independent indicators, which are the computational ability [15] and the memory capacity [16]. The computational ability allows identifying the best laser operating point for achieving the highest performance. It corresponds to the capacity of the system to differentiate two different inputs and gather two identical inputs. More specifically it is defined as the difference between the ranks of two square matrices. Each row is the "value" of one node, taken here as the total power $|E|^2 = |E_x|^2 + |E_y|^2$. Each column is the last time step of a different run of the reservoir. To fill the first matrix, we feed the reservoir with different random inputs for each run. For the second matrix we first feed the reservoir with different random inputs and after 90τ (time for transient to vanish), we feed it with arbitrary chosen inputs which are the same for each run. The computational ability is then a value between 0 and the number of nodes which we normalize between 0 and 1 by dividing by the number of nodes. The normalized quantity allows to compare different architecture with different number of nodes. To have a first idea of the computational ability of our VCSEL-based reservoir, we have run numerical simulations with 400 virtual nodes (Fig. 2) scanning four different parameters: the node interdelay θ, the injection current of the VCSEL μ, the power of the injecting laser P_{inj}, and the feedback strength η.

The results are plotted in Fig. 2 in the θ-μ plane, keeping the same value of the injected power (0.1 mW) and of the

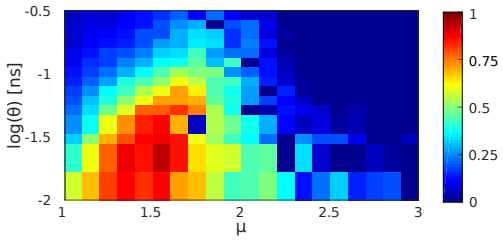

Figure 2: *(color online) Computational ability plot as a function of the injection current μ and the nodes inter-delay θ for an injection power of 0.1 mW and a feedback strength of 10 GHz.*

feedback strength (10 GHz). Figure 2 shows there is a region of parameters in which the computational ability is close to 1, *i.e.* for θ in [0.01 ns, 0.04 ns] and μ in [1.2, 1.5]. We will then keep $\theta = 0.02$ ns for the delay between two nodes, and $\mu = 1.3$ as a value for the injected current for the following tests. We notice that with 400 nodes and $\theta = 0.02$ ns, the delay line is of $8\ ns$. This is comparable to the shortest delay line that has been used in all-optical reservoir computer with the same number of nodes [17].

We also test the computational ability as a function of the feedback strength and the injected power with the two different types of optical feedback described in Eqs. 5-6. This allows us to compare the cases where the VCSEL is emitting along only one polarization mode to the one where the VCSEL is emitting in both orthogonal polarization modes. Indeed, with isotropic feedback, the VCSEL is lasing only along its main polarization axis. The rotated feedback allows to trigger lasing along the depressed axis as well. This is why we will now refer to the isotropic feedback as single-mode reservoir, and to the rotated feedback as the dual-mode reservoir.

Figures 3(a) and (b) show the computational ability of the single-mode and dual-mode reservoir computer, respectively. The region of parameters for which our VCSEL-based reservoir has its highest computational ability, regardless of the feedback configuration. The large region of injection and feedback strength for which the highest computational ability is achieved can be explained by a close inspection into the VCSEL dynamics (not shown here). The lowest performance (darkest blue) occurs when the VCSEL exhibits chaos, whereas the best performance is obtained when the system is in a steady state and for parameters just before the first bifurcation point to periodic dynamics -a condition sometimes referred as "edge of chaos" [18]. The undamping of the relaxation oscillation depends on the injected power and the feedback rate. For instance, for $P_{inj} = 0.1$ mW, the required feedback rate for such dynamics is 31.5 GHz.

The added-value of the dual-mode dynamics is even more evidenced when analyzing the memory capacity, which represents the number of steps in the past the system can remember. The memory capacity is mathematically defined as follows:

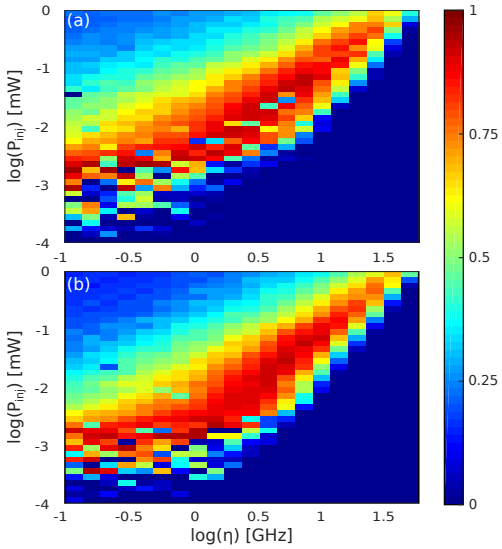

Figure 3: *(color online) Computational ability depending on the injection power P_{inj} and the feedback strength η. (a) single-mode system. (b) dual-mode system*

$$\mu_c = \sum_{i=0}^{\infty} corr\left[y_i(k), u(k-i)\right], \tag{7}$$

where $y_i(k)$ is a reconstruction of $u(k-i)$, which means the reservoir computer is trained in order to get the i^{th} previous input. Theoretically, i should range from 0 to infinity, however, it was shown that the memory of a time-delay reservoir cannot exceed its number of virtual nodes. The maps in Fig. 4 compare the memory capacity of the single-mode and dual-mode reservoir computer. Tests have been performed as previously with 400 nodes, taking for each node $|E|^2$, i.e. the total optical power. We consider 800 samples for the training set and 3200 samples for the testing set.

As in Fig. 3, we have scanned the injected power and the feedback strength and displayed the map of memory capacity for both single-mode and dual-mode reservoirs (Fig. 4). Results show in both configurations a range of parameters for which high memory capacity is achieved. This region of parameters coincides with that of high computational ability. The highest achievable memory depth is approximately 16 steps in the past for the dual-mode system [Fig. 4(b)], which is twice as much as the one reached for the single-mode reservoir (around 8 steps in the past) [Fig. 4(a)]. This is comparable to some of the time-delay all-optical reservoir architectures showing currently the best results in terms of memory [19]. Moreover, considering only $|E_x|^2$ for each node output in the dual-mode system yields the same memory capacity. This highlights that the improved memory capacity is well the result of the polarization mode dynamics induced by the rotating feedback.

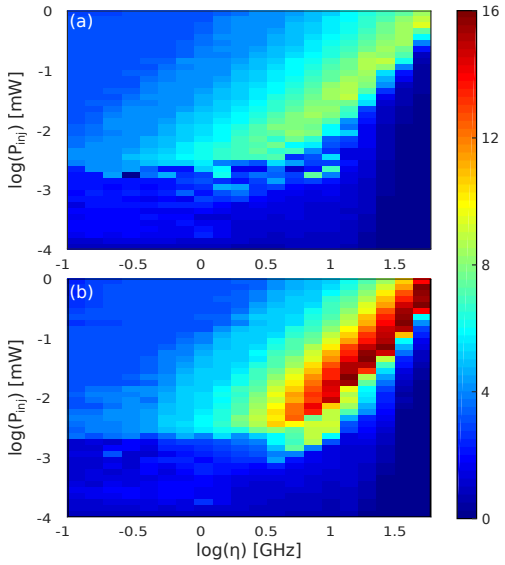

Figure 4: *(color online) Memory capacity depending on the injection power P_{inj} and the feedback strength η. (a) single-mode system. (b) dual-mode system.*

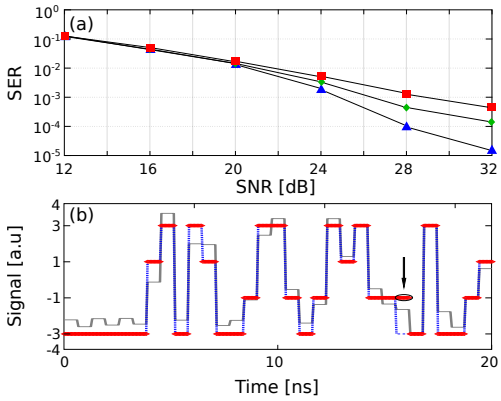

Figure 5: *(color online) Channel equalization. (a) Symbol error rate for different signal-to-noise ratio. □ : single-mode system. ⋄ : dual mode system considering both $|E|^2$. △ : dual-mode system considering $|E_x|^2$ and $|E_y|^2$. (b) Example of reconstruction of a signal with a 24 dB-SNR: the signal sent in the channel (dotted blue), the non-linearly modified signal at the output of the channel (grey), the reconstructed signal (red). The arrow points to the single error in this data sequence*

The previous results suggest an enhancement of the overall computing performance of a VCSEL-based reservoir using the polarization mode dynamics. A more explicit proof is provided when testing our reservoir on a practical task. To this end, we have chosen to test our reservoir with the channel equalization task (Ref. [20]) that has important implications in telecommunications. The objective is to reconstruct from observations $u(i)$ an original signal $d(i)$ after it has propagated through a nonlinear channel. The original signal $d(i)$ is a random sequence of values taken in {-3; -1; 1; 3}. This sequence first goes through a linear channel, which links the output to the input as follows:

$$\begin{aligned} q(i) \quad = \quad & 0.08d(i+2) - 0.12d(i+1) + d(i) + 0.18d(i-1) \\ & -0.1d(i-2) + 0.091d(i-3) - 0.05d(i-4) \\ & +0.04d(i-5) + 0.03d(i-6) + 0.01d(i-7). \end{aligned} \quad (8)$$

Then, the signal is modified using the non-linear function:

$$u(i) = q(i) + 0.026q(i)^2 - 0.11q(i)^3 + v(i), \quad (9)$$

where $v(i)$ is a Gaussian white noise with an adjusted signal-to-noise ratio (SNR) from 12 to 32 dB. Equation (9) gives us the observed data $u(i)$ that are used to infer the corresponding $d(i)$ using reservoir computing.

The reservoir performance on that task is evaluated by the Symbol Error Rate (SER), which is defined as the ratio of the number of false symbols and the total number of symbols. To perform the nonlinear channel equalization at high speed, we have decided to use only 32 virtual nodes, while keeping the same delay between each two nodes $\theta = 0.02$ ns. The delay line is now 0.64 ns, which potentially allows processing speed at 1.5 GSymbols/s. We use as an operating point for our reservoir $\mu = 1.3$, $\eta = 23$ GHz, and $P_{inj} = 0.08$ mW, which corresponds to the highest value of computational ability and memory capacity in both optical feedback configurations. The training is realised with 10,000 samples using a mean square regression. The testing is then realised on 50,000 samples. For each SNR value, the resulting SER is taken as the mean value over 10 different runs. Figure 5 compares the performance of VCSEL-based reservoirs, with single- (□) and dual-mode (⋄) polarization dynamics. In both cases the training considers for each node the total laser power.. The dual-mode reservoir computer achieves better performance compared to the single-mode one: its SER always remains lower than that of the single-mode system. In the highest SNR case, the dual-mode dynamics achieves $SER = 10^{-4}$, hence a reduction by a factor 5 compared to the single-mode case. To maximize the performance, we have also trained the dual-mode reservoir using the power of each polarization mode for each node (△). By doing this, we virtually double the number of node without impacting the length of the delay line, and thus the processing speed. We succesfully reach a $SER = 10^{-5}$ for the highest SNR case, hence another reduction by a factor 10. This is similar to the performance of an opto-electronic reservoir [7], but with a 10000 times higher bit rate. It is also an order of magnitude better than the performance of other all-optical reservoirs [17, 19]. Figure 5(b) shows an example of signal reconstruction, where we highlight the only mis-reconstructed symbol. To evaluate the robustness to noise of our dual-mode reservoir, we have increased the spontaneous emission rate to the realistic value $\beta_{sp} = 4.5 \times 10^{-4}$ ns^{-1}. Our simulations

show that the SER is unchanged. We have also tested the influence of other parameters on the performance of the reservoir. First, we consider the impact of the quantization noise, which is thought sometimes to lower performance on an all-optical reservoir [21]. Here however, accounting for a 8-bit quantization noise improves the memory capacity to 18, but the SER for channel equalization is slightly higher (3×10^{-5} for the 32 dB SNR case). The results may also depend on the feedback phase. For example, the memory capacity reaches 19 with a feedback phase of $\pi/4$ and 18 with a feedback phase of $\pi/2$, but the performance on channel equalization remains the same. Finally, we have also tested the influence of the remaining SFM model parameters by varying e.g. γ_s from 50 GHz to infinity and γ_p from 50 to 200 GHz. The results remain unchanged. This confirms that the increase of performance is mostly attributed to the two mode polarization dynamics induced by the rotating feedback.

We have also tested our dual-mode reservoir with other benchmark tasks such as the Santa Fe prediction task. This test has been performed with the same parameters as the one used for channel equalization task: $\mu = 1.3$, $\theta = 0.02$ ns, $P_{inj} = 0.7$ mW, $\eta = 22$ Ghz, 400 nodes and including the same value for β_{sp}. We successfully reached a normalized mean-square error of 10^{-3}. This is one order of magnitude lower than the numerical results obtained with a similar architecture but using a single-mode edge-emitting laser [22].

In summary, we have studied a reservoir computer, which benefits from the rich and fast polarization dynamics of a VCSEL with optical feedback. We find that the dual-mode dynamics in VCSELs induced by polarization rotated feedback improves the performance of the reservoir computer: it can not only reach high computational performance, but also show a deeper level of memory compared to a single-mode reservoir. This allows the system to show particularly good results very demanding tasks. For example, our VCSEL-based reservoir successfully achieves channel equalization with a SER of 10^{-5} and at a data rate of 1.5 GHz.

Acknowledgements

The authors thank the founders of the Chaire Photonique: Ministère de l'Enseignement Supérieur et de la Recherche, Région Grand-Est, Département Moselle, European Union (FEDER), Metz Métropole, Airbus GDI Simulation, CentraleSupélec, and Fondation CentraleSupélec.

References

[1] J. P. Crutchfield, W. L. Ditto, and S. Sinha, "Introduction to focus issue: Intrinsic and designed computation: Information processing in dynamical systems—beyond the digital hegemony," *Chaos: An Interdisciplinary Journal of Nonlinear Science*, vol. 20, no. 3, p. 037101, 2010. [Online]. Available: https://doi.org/10.1063/1.3492712

[2] H. Jaeger and H. Haas, "Harnessing nonlinearity: Predicting chaotic systems and saving energy in wireless communication," *Science*, vol. 304, no. 5667, pp. 78–80, 2004. [Online]. Available: http://science.sciencemag.org/content/304/5667/78

[3] D. Brunner, M. Jacquot, I. Fischer, and L. Larger, "Photonic networks for neuromorphic computing," p. FTh2E.3, 2017. [Online]. Available: http://www.osapublishing.org/abstract.cfm?URI=FiO-2017-FTh2E.3

[4] K. Vandoorne, P. Mechet, T. Van Vaerenbergh, M. Fiers, G. Morthier, D. Verstraeten, B. Schrauwen, J. Dambre, and P. Bienstman, "Experimental demonstration of reservoir computing on a silicon photonics chip," *Nature communications*, vol. 5, p. 3541, 2014.

[5] L. Appeltant, M. C. Soriano, G. Van der Sande, J. Danckaert, S. Massar, J. Dambre, B. Schrauwen, C. R. Mirasso, and I. Fischer, "Information processing using a single dynamical node as complex system," *Nature Communications*, vol. 2, pp. 468 EP –, Sep 2011. [Online]. Available: http://dx.doi.org/10.1038/ncomms1476

[6] L. Larger, M. C. Soriano, D. Brunner, L. Appeltant, J. M. Gutierrez, L. Pesquera, C. R. Mirasso, and I. Fischer, "Photonic information processing beyond turing: an optoelectronic implementation of reservoir computing," *Opt. Express*, vol. 20, no. 3, pp. 3241–3249, Jan 2012. [Online]. Available: http://www.opticsexpress.org/abstract.cfm?URI=oe-20-3-3241

[7] Y. Paquot, F. Duport, A. Smerieri, J. Dambre, B. Schrauwen, M. Haelterman, and S. Massar, "Optoelectronic reservoir computing," *Scientific reports*, vol. 2, p. 287, 2012.

[8] D. Brunner, M. C. Soriano, C. R. Mirasso, and I. Fischer, "Parallel photonic information processing at gigabyte per second data rates using transient states," *Nature communications*, vol. 4, p. 1364, 2013.

[9] R. M. Nguimdo, G. Verschaffelt, J. Danckaert, and G. V. der Sande, "Fast photonic information processing using semiconductor lasers with delayed optical feedback: Role of phase dynamics," *Opt. Express*, vol. 22, no. 7, pp. 8672–8686, Apr 2014. [Online]. Available: http://www.opticsexpress.org/abstract.cfm?URI=oe-22-7-8672

[10] J. Nakayama, K. Kanno, and A. Uchida, "Laser dynamical reservoir computing with consistency: an approach of a chaos mask signal," *Opt. Express*, vol. 24, no. 8, pp. 8679–8692, Apr 2016. [Online]. Available: http://www.opticsexpress.org/abstract.cfm?URI=oe-24-8-8679

[11] M. Muller, W. Hofmann, T. Grundl, M. Horn, P. Wolf, R. D. Nagel, E. Ronneberg, G. Bohm, D. Bimberg, and M. C. Amann, "1550-nm high-speed short-cavity vcsels," *IEEE Journal of Selected Topics in Quantum Electronics*, vol. 17, no. 5, pp. 1158–1166, Sept 2011.

[12] M. San Miguel, Q. Feng, and J. V. Moloney, "Light-polarization dynamics in surface-emitting semiconductor lasers," *Phys. Rev. A*, vol. 52, pp. 1728–1739, Aug 1995. [Online]. Available: https://link.aps.org/doi/10.1103/PhysRevA.52.1728

[13] M. Virte, K. Panajotov, H. Thienpont, and M. Sciamanna, "Deterministic polarization chaos from a laser diode," *Nature Photonics*, vol. 7, pp. 60 EP –, Nov 2012, article. [Online]. Available: http://dx.doi.org/10.1038/nphoton.2012.286

[14] J. Martin-Regalado, F. Prati, M. S. Miguel, and N. B. Abraham, "Polarization properties of vertical-cavity surface-emitting lasers," *IEEE Journal of Quantum Electronics*, vol. 33, no. 5, pp. 765–783, May 1997.

[15] R. Legenstein and W. Maass, "Edge of chaos and prediction of computational performance for neural circuit models," *Neural Networks*, vol. 20, no. 3, pp. 323 – 334, 2007, echo State Networks and Liquid State Machines. [Online]. Available: http://www.sciencedirect.com/science/article/pii/S0893608007000433

[16] H. Jaeger, "Tutorial on training recurrent neural networks, covering bppt, rtrl, ekf and the" echo state network" approach." GMD-Forschungszentrum Informationstechnik Bonn, 2002, vol. 5.

[17] R. M. Nguimdo, G. Verschaffelt, J. Danckaert, and G. V. der Sande, "Reducing the phase sensitivity of laser-based optical reservoir computing systems," *Opt. Express*, vol. 24, no. 2, pp. 1238–1252, Jan 2016. [Online]. Available: http://www.opticsexpress.org/abstract.cfm?URI=oe-24-2-1238

[18] N. Bertschinger and T. Natschläger, "Real-time computation at the edge of chaos in recurrent neural networks," *Neural Computation*, vol. 16, no. 7, pp. 1413–1436, 2004. [Online]. Available: https://doi.org/10.1162/089976604323057443

[19] F. Duport, B. Schneider, A. Smerieri, M. Haelterman, and S. Massar, "All-optical reservoir computing," *Opt. Express*, vol. 20, no. 20, pp. 22 783–22 795, Sep 2012. [Online]. Available: http://www.opticsexpress.org/abstract.cfm?URI=oe-20-20-22783

[20] J. L. V. John Mathews, "Adaptive algorithms for bilinear filtering," pp. 2296 – 2296 – 11, 1994. [Online]. Available: https://doi.org/10.1117/12.190846

[21] M. C. Soriano, S. Ortín, D. Brunner, L. Larger, C. R. Mirasso, I. Fischer, and L. Pesquera, "Optoelectronic reservoir computing: tackling noise-induced performance degradation," *Opt. Express*, vol. 21, no. 1, pp. 12–20, Jan 2013. [Online]. Available: http://www.opticsexpress.org/abstract.cfm?URI=oe-21-1-12

[22] K. Hicke, M. A. Escalona-Morán, D. Brunner, M. C. Soriano, I. Fischer, and C. R. Mirasso, "Information processing using transient dynamics of semiconductor lasers subject to delayed feedback," *IEEE Journal of Selected Topics in Quantum Electronics*, vol. 19, no. 4, pp. 1 501 610–1 501 610, July 2013.